

Effects of 3d-transition metal doping on the electronic and magnetic properties of one-dimensional diamond nanothread

Zhenzhen Miao(苗珍珍), Can Cao(曹粲), Bei Zhang(张蓓), Haiming Duan(段海明), Mengqiu Long(龙孟秋)

Citation: Chin. Phys. B . 2020, 29(6): 066101 . **doi:** 10.1088/1674-1056/ab84dd
Journal homepage: http://cpb.iphy.ac.cn; http://iopscience.iop.org/cpb

What follows is a list of articles you may be interested in

Growth and doping of bulk GaN by hydride vapor phase epitaxy

Yu-Min Zhang(张育民), Jian-Feng Wang(王建峰), De-Min Cai(蔡德敏), Guo-Qiang Ren(任国强), Yu Xu(徐俞), Ming-Yue Wang(王明月), Xiao-Jian Hu(胡晓剑), Ke Xu(徐科)

Chin. Phys. B . 2020, 29(2): 026104 . **doi:** 10.1088/1674-1056/ab65b9

First-principles study of the band gap tuning and doping control in $CdSe_xTe_{1-x}$ alloy for high efficiency solar cell

Jingxiu Yang(杨竞秀), Su-Huai Wei(魏苏淮)

Chin. Phys. B . 2019, 28(8): 086106 . **doi:** 10.1088/1674-1056/28/8/086106

Delta-doped quantum wire tunnel junction for highly concentrated solar cells

Ali Bahrami, Mahyar Dehdast, Shahram Mohammadnejad, Habib Badri Ghavifekr

Chin. Phys. B . 2019, 28(4): 046102 . **doi:** 10.1088/1674-1056/28/4/046102

Zn-Cu-codoped SnO_2 nanoparticles:Structural, optical, and ferromagnetic behaviors

Syed Zulfiqar, Zainab Iqbal, Jianguo Lü(吕建国)

Chin. Phys. B . 2017, 26(12): 126104 . **doi:** 10.1088/1674-1056/26/12/126104

Dielectric and infrared properties of $SrTiO_3$ single crystal doped by 3d (V, Mn, Fe, Ni) and 4f (Nd, Sm, Er) ions

S. Maletic, D. Maletic, I. Petronijevic, J. Dojcilovic, D. M. Popovic

Chin. Phys. B . 2014, 23(2): 026102 . **doi:** 10.1088/1674-1056/23/2/026102

Effects of 3d-transition metal doping on the electronic and magnetic properties of one-dimensional diamond nanothread*

Zhenzhen Miao(苗珍珍)[1], Can Cao(曹粲)[2], Bei Zhang(张蓓)[1], Haiming Duan(段海明)[1,†], and Mengqiu Long(龙孟秋)[1,2,‡]

[1] *Institute of Low-dimensional Quantum Materials and Devices, School of Physics Science and Technology, Xinjiang University, Urumqi* 830046, *China*
[2] *Hunan Key Laboratory of Super Micro-structure and Ultrafast Process, School of Physics and Electronics, Central South University, Changsha* 410083, *China*

(Received 27 February 2020; revised manuscript received 26 March 2020; accepted manuscript online 31 March 2020)

The diamond nanothread (DNT), a new one-dimensional (1D) full carbon sp^3 structure that has been successfully synthesized recently, has attracted widespread attention in the carbon community. By using the first-principles calculation method of density functional theory (DFT), we have studied the effects of 3d transition metal (TM) atomic doping on the electronic and magnetic properties of DNT. The results show that the spin-polarized semiconductor characteristics are achieved by doping Sc, V, Cr, Mn, and Co atoms in the DNT system. The magnetic moment ranges from 1.00 μ_B to 3.00 μ_B and the band gap value is from 0.35 eV to 2.54 eV. The Fe-doped DNT system exhibits spin-metallic state with a magnetic moment of 2.58 μ_B, while the Ti and Ni-doped DNT systems are nonmagnetic semiconductors. These results indicate that the 3d TM atoms doping can modulate the electronic and magnetic properties of 1D-DNT effectively, and the TM-doped DNT systems have potential applications in the fields of electronics, optoelectronics, and spintronics.

Keywords: diamond nanothread, transition metal atom, doping, electronic and magnetic property

PACS: 61.46.–w, 62.23.Hj, 71.20.–b, 75.75.–c **DOI:** 10.1088/1674-1056/ab84dd

1. Introduction

In the past few decades, carbon-based nanomaterials have been extensively studied in the scientific community for their unique and fascinating physical and chemical properties, many new carbon allotropes, such as fullerenes (C_{60}),[1,2] carbon nanotubes (CNTs),[3] graphene,[4,5] and graphyne,[6,7] have been added to the family of carbon. In 2015, Fitzgibbons *et al.*[8] successfully synthesized a new carbon nanomaterial through the high-pressure solid state reaction of benzene: diamond nanothread (DNT), which successfully became the newest member of the carbon family. Its surface is functionalized by hydrogen, the C:H ratio is 1 : 1, the C–C bond is a closely packed sp^3 hybrid, and the carbon atoms are arranged in a rhombohedral tetrahedral pattern.[9] The term "nanothread" emphasizes its ultra-small diameter, which represents ideal one-dimensional (1D) material.[10] According to molecular dynamics simulations, DNT has excellent mechanical properties and thermal stability than other carbon nanostructures, which ideal strength is 26.4 nN (134 GPa), Young's modulus is 850 GPa, and specific strength and stiffness are 4.13×10^7 N·m/kg and 2.6×10^8 N·m/kg, respectively.[11–14] And the thermal stability of DNT shows that when the system is heated to 300 °C–400 °C, its characteristic structure will not change over a long period of time, and its mechanical strength can be retained even after 1%–2% hydrogen analysis.[15] The excellent properties of the DNT system indicate its great potential in the development of lightweight and strong materials.

As a new sp^3-hybridized 1D nanomaterial, DNT has high strength and thermal stability.[14,16–18] However, the wideband gap ($\sim$ 3.9 eV) of DNT prevents applications in the field of electronics.[9] Traditionally, a common method of modifying the electronic properties of a material is to dope with foreign atomic species. For example, carbon nanotubes are doped via an alkali metal atom (Li or K) to cause charge transfer between an alkali metal atom and the carbon host.[19–21] Modulation of the electronic structure of boron nitrogen nanotube (BNNT) has been substantially achieved by doping the BNNT with the metal atoms Au, Al, Pt, Ti, and V.[22–25] By N-doping, the zigzag graphene nanoribbon (ZGNR) can be a spin gapless semiconductor from an antiferromagnetic semiconductor, and the energy level is changed.[26,27] Since magnetic nanostructure is an important research field in science and technology, researchers have conducted extensive study on magnetic materials by doping atoms. For example, the spontaneous magnetization of the system is achieved by replacing the boron or nitrogen atoms of the BNNTs with magnetic transition metal (TM) atoms.[28,29] The substitution of the TM atom on the phosphorene or molybdenum disulfide (MoS_2), which will cause magnetization in the system.[30–35]

Owing to the metal atoms have different electronic and magnetic properties, the structure, electronic, and magnetic properties of the metal-doped DNT system are intriguing and still not well understood. Moreover, the substitution doping is of great significance for the development of nanoelectronic

*Project supported by the National Natural Science Foundation of China (Grant Nos. 21673296 and 11664038) and the Natural Science Foundation of Xinjiang Uygur Autonomous Region of China (Grant No. 2019D01C038).

†Corresponding author. E-mail: dhm@xju.edu.cn
‡Corresponding author. E-mail: mqlong@csu.edu.cn

© 2020 Chinese Physical Society and IOP Publishing Ltd

devices.[36,37] Therefore, in this study, we have carried out a systematic study on the substitution of a single C atom in DNT by different transition metal (TM) atoms within density functional theory (DFT). Our results show that doping TM atoms can affect the electronic and magnetic properties of DNT. The rest of the paper is organized as follows. In Section 2, we detail the computational methods of the first principles calculations and the models of the TM atoms-dopped DNTs. The electronic and magnetic properties of the TM-doped DNTs are investigated in Section 3. The conclusions are given in Section 4.

2. Computational methods

In this research, our calculations are performed with DFT as implemented in Vienna *ab initio* simulation package (VASP),[38–40] adopting a generalized gradient approximation (GGA)[41] for the exchange–correlation potential. The ion–electron interaction is treated with the projected-augmented wave (PAW), and the plane wave cutoff energy for the wave function is set to 500 eV. The actual DNT unit cell has a lattice constant of 4.3 Å. We use a rectangular supercell with a size of 20 Å×20 Å×8.6 Å. With the length of c in the axial or z direction[42] being twice of the periodicity of the original DNT. The supercell contains four layers of atoms in the direction of the tube axis, giving a total of 64 atoms in the supercell, which is selected as the model. A single carbon atom in the edge of the DNT is replaced by a TM atom to form a TM-doped DNT. Considering the periodic boundary condition, the closest distance between the two DNTs is no less than 15 Å to avoid possible coupling between the TM in the parallel direction of the DNT. The criterion of convergence for structure relaxation is the change of total energy less than 10^{-6} eV and the residual force on atom less than 0.001 eV/Å. The reciprocal space is sampled by a fine grid of $1\times1\times13$ k-point in the Brillouin zone, respectively.

3. Results and discussions

3.1. Geometry of TM-doped DNTs

The TM-doped DNT system is constituted by replacing a single C atom in the edge of the DNT with a TM atom, as shown in Fig. 1. After relaxation, the local symmetry of the 3d TM-doped DNT is destroyed under Jahn–Teller distortion,[43] resulting in slight deformation of the system. The lattice constant, bond length, and bond angle of the 3d TM-doped DNT structure are presented in Table 1, respectively. We can find that the equilibrium lattice constants of the 3d TM-doped DNTs systems are between 8.65 Å–8.72 Å. Compared to the pure DNT system, since the doped metal atom size is larger than that of the C atom, the lattice constant value of the doped DNT is larger than that of the pure DNT (8.60 Å). And for the bond length and bond angle values between the 3d TM atom and its adjacent carbons in the doped DNT system, it can be clearly seen that, owing to the radius of the 3d TM atom is larger than that of the substituted C atom, all TM-C bond lengths ($D_{\mathrm{TM-C}}$) in the 3d TM-doped DNTs system are longer than the C–C bond length (1.570 Å) of the pure DNT system, while the bond angles are smaller than the average bond angle (110.296°) of the pure DNT system. Among them, the average bond length value of the Sc-, Ti-, Cu-, and Zn-doped DNTs system is around 2.00 Å, and the corresponding average bond angle is between 85°–90°. For the Fe-doped DNT system, we can see the bond length value is about 1.87 Å and bond angle value is about 103°, which have the smallest difference from the pure DNT. These results of the changes in bond length and bond angle indicate that there is structural distortion around the 3d TM impurity in the doped DNTs, as shown in Fig. 1.

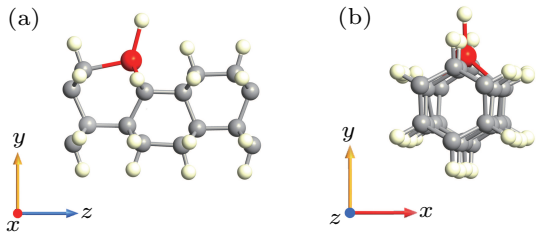


Fig. 1. The geometry is optimized for the 3d TM-doped DNTs: (a) front, and (b) side view of the doped DNT. The grey and white balls refer to C and H atoms, and the red ball refers to the doping atoms, including Sc, Ti, V, Cr, Mn, Fe, Co, Ni, Cu, and Zn, respectively.

To analyze the stability of the doping configurations, we calculated the formation energy E_{f} of the 3d TM-doped DNTs, which is defined as follows:

$$E_{\mathrm{f}} = E_{(\mathrm{doped})} - [E_{(\mathrm{pure})} + n\mu_{(\mathrm{TM})} - m\mu_{(\mathrm{C})}], \tag{1}$$

where $E_{(\mathrm{doped})}$ is the total energy of the 3d TM-doped DNT system, $\mu_{(\mathrm{C})}$ is the chemical potential of the C atom, $\mu_{(\mathrm{TM})}$ is the chemical potential of the isolated 3d TM atom, $E_{(\mathrm{pure})}$ is the energy of pristine DNT, and n, m represent the number of doped TM atoms and substituted C atoms, respectively.[36,44] The corresponding calculated E_{f} of these TM atom-doped DNTs is shown in Table 2. Among them, we can find that there are positive formation energies for the Cu- and Zn-doped DNTs, and the corresponding values are 1.986 eV and 3.770 eV, respectively. In addition, the other 3d TM-doped DNTs have negative formation energies and the negative maximum is −2.22 eV for the Ti-doped DNT system. According to the fact that the positive value of the formation energy is endothermic and the negative value is exothermic. Compared with the Cu- and Zn-doped DNT system, other 3d TM-doped DNT systems would be more stable. Furthermore, it can also be seen from the formation energy in Table 2 that other TM atoms are good substitution for the C in the DNT because they can be well combined with the doped structure. Therefore, in the following calculations, we have considered only the DNT systems doped with other 3d TM atoms (except Cu and Zn dopings).

Table 1. Lattice constant of an atom replaced by a transition metal (TM) atom in the DNT, the bond length and the corresponding bond angle between TM and its three nearest neighbor C atoms.

Structure	Lattice constant/Å	D_{TM-C}/Å			Angle/(°)		
Pure	8.60	1.570	1.545	1.545	112.069	112.069	106.751
Sc	8.70	2.203	2.133	2.381	93.215	87.623	75.601
Ti	8.69	2.031	2.061	2.061	92.682	96.399	92.688
V	8.70	1.952	2.014	2.014	93.39	88.884	93.392
Cr	8.71	1.952	1.977	1.977	98.391	94.393	98.391
Mn	8.67	1.960	1.985	1.985	93.304	86.372	93.323
Fe	8.70	1.874	1.872	1.872	105.015	100.554	105.012
Co	8.65	1.889	1.897	1.897	97.622	91.420	97.624
Ni	8.65	1.926	1.926	1.826	95.864	82.255	95.841
Cu	8.66	1.920	2.127	2.128	89.946	85.546	90.028
Zn	8.71	2.065	2.211	2.211	89.936	81.820	89.938

Table 2. Formation energy and band gap of the 3d TM-doped DNT systems and pure DNT system.

Structure		Pure	Sc	Ti	V	Cr	Mn	Fe	Co	Ni	Cu	Zn
E_f/eV		–	−0.48	−2.22	−1.20	0.05	−0.03	−0.57	−1.14	−0.77	1.99	3.77
Band gap/eV	up	3.93	1.17	2.45	0.35	1.45	1.71	–	0.73	1.79	0.73	1.62
	down	3.93	1.28	2.45	2.41	2.06	2.54	–	0.56	1.79	0.56	–

3.2. Electronic structures

The spin-dependent electronic structures of 3d TM-adsorbed DNTs are plotted in Fig. 2. The previous study has demonstrated that the pure (3,0) DNT is a direct band gap semiconductor with a band gap of 3.92 eV.[10] After TM atoms are doped, the band gap is significantly reduced, which makes the carrier concentration increase, and a flat band gap appears at the Fermi level (FL). Because the transition metal atoms are doped, the outermost electrons of the metal atoms will be transferred, which changes the overall charge properties of the DNT system. The internal charge of the DNT system is reorganized, and the overall energy level will be relatively displaced. As shown in Figs. 2(a)–2(h), we can find that the band structures of the TM-doped DNTs substantially depend on the specific impurity atoms. Firstly, it is seen that the spin-up and spin-down states are degenerated in the Ti- and Ni-doped systems, and a direct band gap of 2.45 eV and 1.78 eV can be observed respectively, becoming markedly narrower than that of the pure DNT. Then, we observed that both the spin-up and the spin-down states across the FL in Fig. 2(f), which indicates that the Fe-doped system behaves the spin-splitting metallic property, as displayed in the plug-in of Fig. 2(f). Thirdly, with regard to Sc-, V-, Cr-, Mn-, and Co-doped DNTs systems, we can find that the spin-splitting semiconductor properties, and the spin-up (spin-down) band gap values are in the range of 0.35 eV–1.71 eV (0.56 eV–2.54 eV), which would be useful in spintronic applications. From the above analyses, we can conclude that the doping of 3d TM atoms can modulate the band gap of the DNT system effectively, and transforming the DNT conversion from metal characteristics to spin-splitting semiconductor characteristics.

From the band structure we can also find that the spin-up and spin-down states of the 3d TM-doped DNTs system are non-degenerate (except Ti- and Ni-doped DNTs systems) with spin polarization generation. The 3d TM atom is doped with the DNTs system, and the impurity band is introduced in the band structure to reduce the band. In order to further understand the electronic structure and reveal the origin of magnetism, figure 3 shows the partial density of states (PDOS) of the TM atom and its three C atoms (C3) connected to the TM atom. As can be seen from Figs. 3(a)–3(b), the PDOS peaks of Sc- and Ti-doped DNTs are primarily composed of the TM 3d states and also contain some C3 2p states near FL. As shown for the Sc-doped DNT system, an interaction can be seen between 3d orbital of Sc atoms and 2p orbital of C3 atoms. Therefore, we conclude that the magnetic moment of the doped DNT system would be originated from the polarization of TM 3d electrons and C3 2p electrons. For the V-, Cr-, Mn-, Fe-, Co-, and Ni-atoms-doped DNT systems, as can be seen in Figs. 3(c)–3(h), it is clearly seen that the PDOS is mainly provided by the 3d orbital of the metal atom at the FL. In the case of Ti and Ni doping, figures 3(b) and (3h) show a symmetrical PDOS for spin-up and spin-down states below the FL indicating the nonmagnetic phenomenon. Moreover, we also studied the d electron distribution at the FL in Fig. 3. In spin-polarized systems, we found that the major source of spin polarization of each TM atom originated from different d orbitals. For instance, the major contribution to the magnetic moment in Mn doping stems from the d_{x^2} orbital. In the V-doped system, mostly the d_{xz} and d_{x^2} orbitals are the major source of spin polarization. In Cr and Fe doping, three different orbitals such as d_{xz}, d_{x^2}, and d_{yz} give rise to the magnetic moment of the Cr and Fe atoms. These results correspond with the calculated band structures and spin densities.

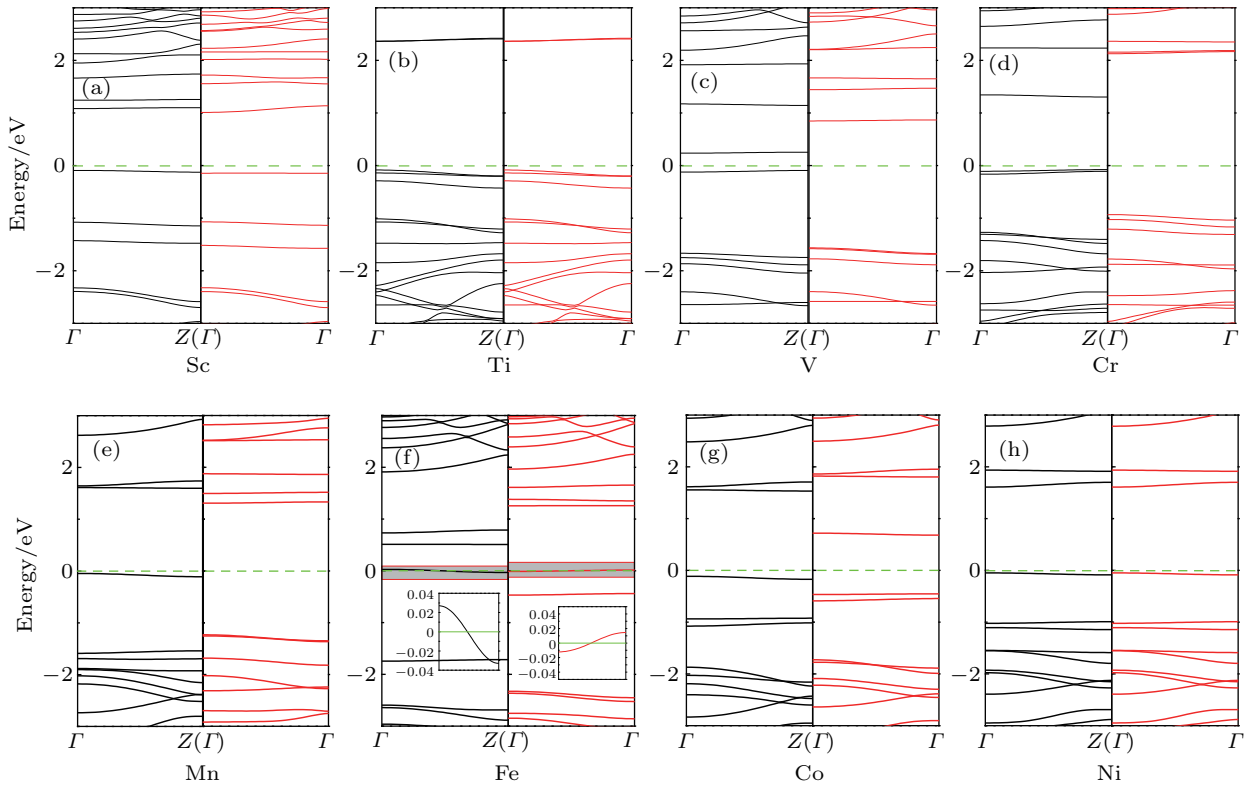


Fig. 2. Electronic structures of different 3d TM atom-doped DNT, panels (a)–(h) refer to Sc, Ti, V, Cr, Mn, Fe, Co, Ni, respectively. The black and red lines describe the spin-up and spin-down bands.

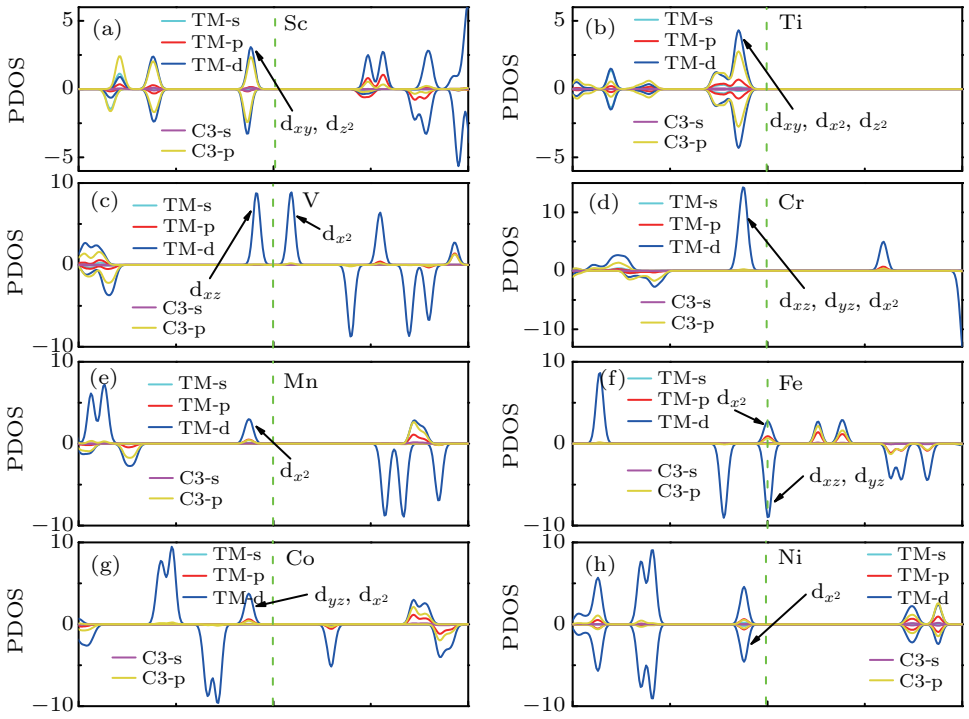


Fig. 3. Calculated partial density of states (PDOS) of the 3d TM atom and its nearest-neighbor C atom for each substitutional doped DNT: (a) Sc-DNT, (b) Ti-DNT, (c) V-DNT, (d) Cr-DNT, (e) Mn-DNT, (f) Fe-DNT, (g) Co-DNT, (h) Ni-DNT. The FL is set to zero energy and indicated by the vertical green dashed line.

3.3. Magnetic properties

The magnetic moments of the TM-doped DNTs are depicted in Fig. 4. The magnetic moments of the TM-doped DNTs should mainly originate from the doped TM impurities, since the ground states of the pristine DNT are nonmagnetic. As the atomic number increases, the variation of magnetic moment in Fig. 4 can be divided into three categories. Firstly, the magnetic moments of Ti- and Ni-doped systems

are zero. Secondly, the magnetic moments of the Cr-, Mn-, and Fe-substituted systems are larger than 1 μ_B. Particularly, the magnetic moment of the Mn substituted system is the maximum (3 μ_B) owing to the outermost valence electron of the Mn atom is half full. Thirdly, for the Sc-, V-, and Co-doped systems, the magnetic moment appears as a fixed value (1 μ_B). Furthermore, we find that most of the TM-doped DNTs exhibit a magnetic moment, which is mainly due to the local magnetic moment of the doped atoms caused by the strong spin polarization.

In order to obtain insight into the magnetic origin, we have calculated the spin density diagram for the 3d TM-doped DNTs as displayed in Fig. 5. From Fig. 5, we notice that the magnetism is mainly attributed to the TM atom with a strong localized magnetic moment. First of all, it is hardly any spin density can be observed for the Ti- and Ni-doped DNT systems. Then, For the V-, Cr-, Mn-, and Fe-doped DNTs systems, the TM and its adjacent C3 atoms provide most of magnetic moments in the spin-up state, while the C3 atoms around the doped Cr and Mn atoms provide spin-down state. Thirdly, in Sc-doped DNT system, it can be seen that in addition to the metal atom, the C3 atoms connected to the metal atoms also provide spin density and have contributions to the magnetic moment.

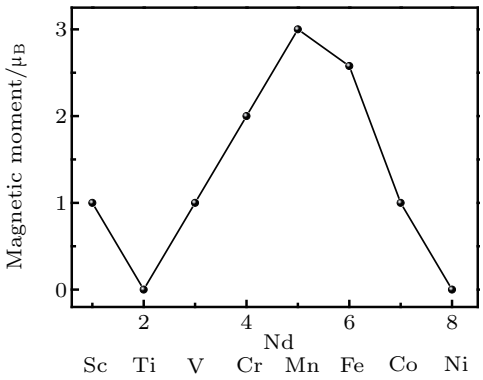


Fig. 4. Magnetic moments of the 3d series TM atoms substituted DNT as a function of the number of valence electrons.

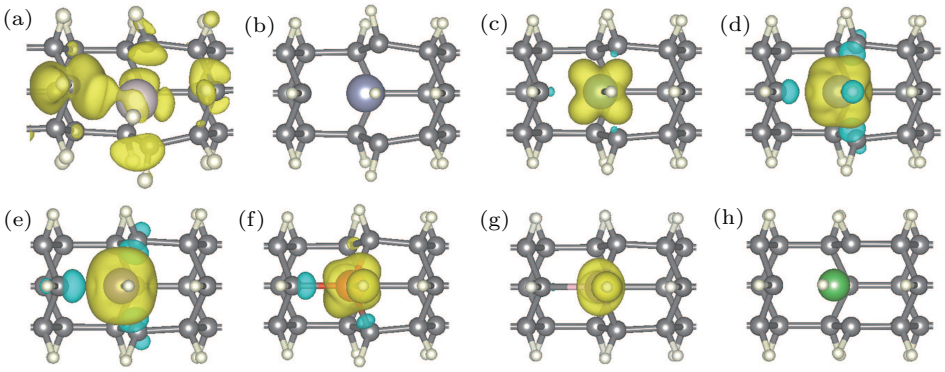


Fig. 5. Spin density for single TM substitutionally doped DNT systems. Top and side views of (a) Sc-DNT, (b) Ti-DNT, (c) V-DNT, (d) Cr-DNT, (e) Mn-DNT, (f) Fe-DNT, (g) Co-DNT, (h) Ni-DNT. Yellow and blue represent spin-up and spin-down, respectively. The isosurface is taken as 0.0002 e/Å^3 for panel (a); and 0.01 e/Å^3 for panels (b)–(h).

4. Conclusions

In summary, based on the first-principles study of the density functional theory, the effects of TM atomic doping on the electronic and magnetic properties of DNT were investigated. Our results show that the TM atom doping retains the original band gap characteristics in the spin-polarization state except the impurity band near the FL. For Sc-, V-, Cr-, Mn-, and Co-doped DNT systems, the characteristics of the spin-polarized semiconductor are realized. The magnetic moments are in the range from 1.00 μ_B to 3.00 μ_B, wherein the maximum magnetic moment is generated by doping Mn atom in the DNT system, and the spin-up (spin-down) band gap value ranging from 0.35 eV to 1.71 eV (0.56 eV to 2.54 eV). The Fe-doped DNT system exhibits metallic state with a magnetic moment of 2.58 μ_B, while the Ti- and Ni-doped DNTs systems are nonmagnetic semiconductors. These results have demonstrated that the doping of 3d TM atoms can reduce the band gap value of the DNT system and have potential to generate spin polarization, thereby, providing a viable mean for designing materials in electronic and spintronics devices.

References

[1] Liu J, Rinzler A G, Dai H, Hafuer J H, Bradley R K, Boul P J, Lu A, Iverson T, Shelimov K, Huffman C B, Rodriguez-Macias F, Shon Y S, Lee T R, Colbert D T and Smally R E 1998 *Science* **280** 1253
[2] Kroto H W, Heath J R, O'Brien S C, Curl R F and Smalley R E 1985 *Nature* **318** 162
[3] Xia Y, Yang P, Sun Y, Wu Y, Mayers B, Gates B, Yin Y, Kim F and Yan H 2003 *Adv. Mater.* **15** 353
[4] Zhang D, Long M Q, Zhang X, Ouyang F, Li M and Xu H 2015 *J. Appl. Phys.* **117** 014311
[5] Zhang H 2015 *ACS Nano* **9** 9451
[6] Peng D D, Zhang X J, Li X B, Wu D and Long M Q 2018 *J. Appl. Phys.* **124** 184303
[7] Long M Q, Tang L, Wang D, Li Y L and Shuai Z 2011 *ACS Nano* **5** 2593
[8] Fitzgibbons T C, Guthrie M, Xu E S, Crespi V H, Davidowski S K, Cody G D, Alem N and Badding J V 2015 *Nat. Mater.* **14** 43
[9] Stojkovic D, Zhang P and Crespi V H 2001 *Phys. Rev. Lett.* **87** 125502
[10] Wu W, Bo T, Shan G, Yang S A and Gang Z 2018 *J. Phys. Chem. C* **122** 3101
[11] Silveira J F R V and Muuiz A R 2017 *Carbon* **113** 260

[12] Feng C, Xu J, Zhang Z and Wu J 2017 *Carbon* **124** 9
[13] Xiao J, Chen M M, Liu W J, He J, Pan C N and Long M Q 2019 *Physica E* **111** 37
[14] Podlivaev A I and Openov L A 2017 *Semiconductors* **51** 636
[15] Openov L A and Podlivaev A I 2016 *JETP Lett.* **104** 193
[16] Zhan H, Gang Z, Zhang Y, Tan V B C, Bell J M and Gu Y 2016 *Carbon* **98** 232
[17] Zhan H, Gang Z, Bell J M and Gu Y 2016 *Carbon* **107** 304
[18] Zhu T and Ertekin E 2016 *Nano Lett.* **16** 4763
[19] Zhao J, Buldum A, Han J and Ping L J 2000 *Phys. Rev. Lett.* **85** 1706
[20] Jing L and Nagase S 2004 *Phys. Rev. B* **69** 205304
[21] Jo C, Kim C and Lee Y H 2002 *Phys. Rev. B* **65** 035420
[22] Mirzaei M and Nouri A 2010 *J. Mol. Struct. Theochem.* **942** 83
[23] Dong Q, Li X M, Tian W Q, Huang X R and Sun C C 2010 *J. Mol. Struct. Theochem.* **948** 83
[24] Durgun E, Jang Y R and Ciraci S 2007 *Phys. Rev. B* **76** 73413
[25] Yao K L, Min Y, Zhu S C, Gao G Y, Liu Z L and Cheng H G 2008 *Phys. Lett. A* **372** 5609
[26] Li Y F, Zhou Z, Shen P W and Chen Z F 2009 *ACS Nano* **3** 1952
[27] Shan S Y, Wei T Z and Jiang Q 2010 *IEEE T. Nanotechnol.* **9** 78
[28] He K H, Zhang G, Chen G, Wan M and Ji G F 2008 *Physica B* **403** 4213
[29] Li X M, Wei Q T, Qi D, Huang X R, Sun C C and Lei J 2011 *Comput. Theor. Chem.* **964** 199
[30] Yang G, Xu S, Wei Z, Ma T and Wu C 2016 *Phys. Rev. B* **94** 075104
[31] Jiang J, Wang X and Yan S 2018 *Comput. Mater. Sci.* **153** 10
[32] Luo Y, Ren C, Wang S, Li S, Zhang P, Yu J, Sun M, Sun Z and Tang W 2018 *Nanoscale Res. Lett.* **13** 282
[33] Babar R and Kabir M 2016 *J. Phys. Chem. C* **120** 14991
[34] Yu W, Zhu Z, Niu C Y, Li C J Cho H and Jia Y 2016 *Nanoscale Res. Lett.* **11** 77
[35] Andriotis A N and Menon M 2014 *Phys. Rev. B* **90** 125304
[36] Li Y J, Li S L, Gong P, Li Y L, Fang X Y, Jia Y H and Cao M S 2018 *Physica E* **104** 247
[37] Lia Y H, Gong P, Li S L, Ma W H, Fang X Y, Yang Y Y and Cao M S 2020 *Phys. Lett. A* **384** 126106
[38] Kresse G and Joubert D 1999 *Phys. Rev. B* **59** 1758
[39] Kresse G 1995 *J. Non-Cryst. Solids* **192-193** 222
[40] Kresse G and Furthmülle J 1996 *Phys. Rev. B* **54** 11169
[41] Sun M L, Slanina Z and Lee S L 1995 *Chem. Phys. Lett.* **233** 279
[42] Li Y L, Gong P and Fang X Y 2020 *Chin. Phys. B* **29** 037304
[43] Ma Y, Lehtinen P O, Foster A S and Nieminen R M 2004 *New J. Phys.* **6** 68
[44] Stern R, Dongre B and Madsen G K H 2016 *Nanotechnology* **27** 334002